Bulky PNP ligands blocking metal-ligand cooperation allow for isolation of Ru(0), and lead to catalytically active Ru complexes in acceptorless alcohol dehydrogenation

Shubham Deolka[1]; Robert R. Fayzullin[2]; Eugene Khaskin[1,*]

1. Okinawa Institute of Science and Technology Graduate University, 1919-1 Tancha, Onna-son, Kunigami-gun, Okinawa, Japan, 904-0412 2. Arbuzov Institute of Organic and Physical Chemistry, FRC Kazan Scientific Center, Russian Academy of Sciences, 8 Arbuzov Street, Kazan 420088, Russian Federation

KEYWORDS Ruthenium, metal-ligand cooperation, alcohol dehydrogenation, acceptorless dehydrogenation, catalysis.

ABSTRACT: We synthesized two 4Me-PNP ligands which block metal-ligand cooperation (MLC) with the Ru center and compared their Ru complex chemistry to their two traditional analogues used in acceptorless alcohol dehydrogenation catalysis. The corresponding 4Me-PNP complexes, which do not undergo dearomatization upon addition of base, allowed us to obtain rare, albeit unstable, 16 electron mono CO Ru(0) complexes. Reactivity with CO and H_2 allows for stabilization and extensive characterization of bis CO Ru(0) 18 electron and Ru(II) cis and trans dihydride species that were also shown to be capable of C(sp^2)-H activation. Reactivity and catalysis are contrasted to non-methylated Ru(II) species, showing that an MLC pathway is not necessary, with dramatic differences in outcomes during catalysis between ^{i}Pr and ^{t}Bu PNP complexes within each of the 4Me and non-methylated backbone PNP series being observed. Unusual intermediates are characterized in one of the new and one of the traditional complexes, and a common catalysis deactivation pathway was identified.

INTRODUCTION

Ruthenium complex catalyzed acceptorless dehydrogenative coupling of alcohols to esters and the reverse hydrogenation of esters performed under H_2 pressure is now a commonly established reaction since its description under mild conditions by Milstein in 2005/6 (Eq. 1). [1]

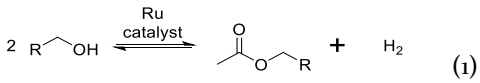

(1)

Since those reports, similar Ru pincer complexes have been reported to be active in a number of related reactions such as: the synthesis of amides from alcohols and amines[2] and the reverse reaction;[3] synthesis of imines;[4] amines from alcohols;[5] acceptorless transformation of alcohols to carboxylic acids;[6] CO_2 reduction;[7] thioester synthesis;[8] deuteration of alcohols;[9] cross coupling of alcohols;[10] and the introduction of alcohols as a substrate in reactions normally requiring aldehydes,[11] sometimes enabling novel reactivity. [12] Ideally, all these reactions can be used in the synthesis of bulk chemicals, or for pharmaceutical intermediates and fine chemicals in the chemical industry.

The promiscuity of the catalysts often comes with the major drawback of non-selectivity and undesired side reactions with functional groups. The design of catalytic systems that work at temperatures and pressures close to ambient conditions and improve selectivity is a major goal of current research efforts. In ester hydrogenation, this has already led to recent reports of complexes that are highly active at temperatures of <100°C and can achieve at least several thousand turnovers.[13]

Concurrently, the mechanism of these transformations continues to be examined in detail.

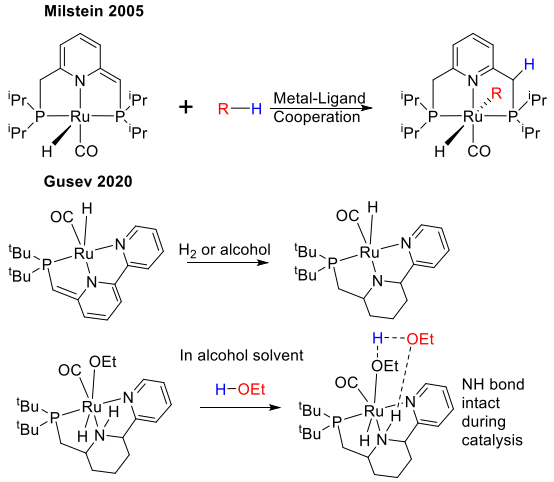

SCHEME 1. Proposed MLC mechanism contrasted to ligand assisted substrate activation

Some of the first crucial steps of the original Milstein system's catalytic cycle are believed to be dearomatization of the central pyridine ring after deprotonation by base, and re-aromatization by substate addition across the ligand arm and metal center (i.e. Metal-Ligand Cooperation or MLC) (Scheme 1). [1d,14]

A number of recent studies have found that pyridine supported Ru complexes can hydrogenate the pyridine ring during catalysis, forming a Noyori-type catalyst with an NH functionality.[15] This included our recent report on a Milstein group developed bipy-PNN complex that can catalyze ester hydrogenation and several related transformations.[16] We showed that the central ring can undergo facile hydrogenation either in the presence of alcohols or hydrogen gas (Scheme 1 middle). DFT calculations suggested that catalysis proceeds via a metal-ligand assisted mechanism on a coordinatively saturated 18e$^-$ species, through a hydrogen bond network between the NH functionality and the metal bound substrate (Scheme 1 bottom). During this process, the NH bond remains intact.

When we modified the PNP ligand used in the original Milstein report by a pendant pyridine unit (Scheme 2 top), we were surprised to see a complete shutdown of catalytic activity, which was caused by a rearrangement of the backbone ligand skeleton and tighter binding of the pendant pyridine.[17]

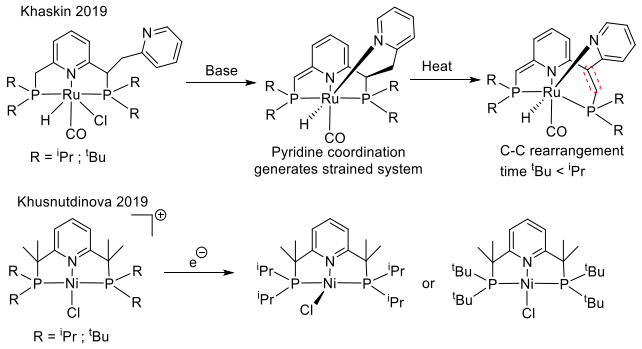

SCHEME 2. Earlier reported backbone PNP pincer modified systems

Another modification of the PNP ligand undertaken in our group involved synthesizing bulky, tetramethyl ligands (Scheme 2 bottom) that stabilized low oxidation state nickel complexes that cannot be observed with a normal, non-methylated PNP ligand. [18] Such drastic differences in reactivity arising from slight modifications of ligand architecture suggest that it may be possible to discover a superior PNP pincer-based Ru catalyst. In this regard, the commercially available MACHO Ru PNP catalyst that does away with the pyridine in lieu of a flexible alkyl backbone is one of the best performing catalysts on the market today.[19]

After obtaining such unusual results with the original bipyPNN-Ru complex and the pyridyl modified PNP Ru complex, we decided to test the 4Me-PNP ligand on Ru and compare its reactivity to the original non-methylated system (Scheme 1 top). Based on the earlier Ni chemistry results, we expected that the 4Me-PNP ligand may form Ru(0) complexes, however, we did not expect this ligand to undergo rearrangement like the pyridyl modified PNP. If the Ru(0) complexes should be stable, they would be a relatively rare example of a pincer Ru(0) species and may provide a new and unique mechanism for alcohol dehydrogenation.

Recently, the CaRLa group found that a Ru(0) complex formed by the decomposition of the commercially available MACHO Ru catalyst was capable of interconverting to a catalytically active Ru(II) species, highlighting the possible role of Ru(0) as a resting state or intermediate in catalysis.[20]

An ^{i}PrPNP-Ru complex was in the original Milstein report in 2005,[1a] which tested only two pincer complexes for the dehydrogenative coupling of alcohols. The best performing catalyst was determined to be a diethylamine PNN complex (now commercially available from Aldrich), which has recently been shown by Chianese to form a Noyori-type species in the presence of strong ligands during catalysis. [21] The other tested complex was the symmetrical PNP Ru(II) complex, and it also behaved as a highly competent catalyst. Unfortunately, it was not further explored due to slightly inferior activity after its one trial run.

However, our group was uniquely positioned to revisit the reactivity of that complex and compare it to its methylated version. We synthesized the two previously reported pyridine-based PNP ^{i}Pr and ^{t}Bu complexes **1** and **2** using the procedure of Scheme 3, and made tetramethyl analogues **3** and **4** where MLC is blocked as the pyridine ring cannot become dearomatized (4Me-PNP).

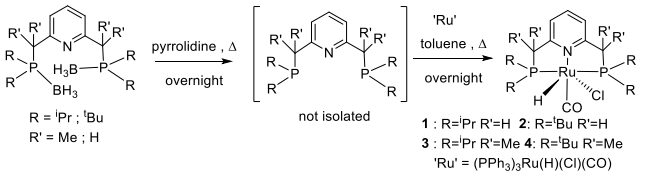

SCHEME 3. Synthesis of PNP and 4Me-PNP supported complexes.

In the current paper, we show that we were able to access Ru(0) complexes with the 4Me-PNP ligands and stabilize them for X-ray characterization by subsequent addition of CO gas. H_2 addition to deprotonated PNP and 4Me-PNP complexes gave trans-H_2 for the former and cis-H_2 for the latter, suggesting that MLC matters for the activation of substrates such as hydrogen gas. The 4Me-PNP based complexes were also capable of H/D exchange between the C_6D_6 solvent and the dissolved H_2 gas via the metal hydrides at relatively mild (> 60°C) temperatures. H/D exchange between solvent and substrate via Ru(II) CH activation has been observed previously by Periana[22] and

Grubbs.[23] Gunnoe also observed deuteration of Ru coordinated ligands by arene NMR solvents with a complex supported by a trispyrazolylborate ligand.[24] However, we did not focus on this reactivity in the current report, as it was attendant to the exploration of acceptorless alcohol dehydrogenation catalysis.

We found that all complexes were active in alcohol dehydrogenation catalysis, but no clear trend could be discerned, and the most active complex was the bulkiest **4**. A detailed study of the reactivity in benzene solutions spiked with ethanol, and in neat ethanol solvent, allowed us to isolate unusual catalytic intermediates for complexes **2** and **4**, and to identify acetate complexes, formed via a Guerbet disproportionation of the alcohol substrate, as a deactivation pathway for catalysis.

RESULTS and DISCUSSION

Structural Data Comparison

In order to observe the steric influence of the four extra methyl groups on the system, we crystallized and measured data for starting complexes **1-4** (Figure 1; the X-ray structure of complex **2** was published previously [25]), Comparing the structures revealed that the least bulky complex **1** is a staggered propeller between the pyridine and the P-Ru-P plane, with the bulkier species adopting an increasing butterfly shape, seen by comparing the angles made by the para carbon of the pyridine, the nitrogen, and the Ru center. The Ru-P and Ru-H bonds are slightly elongated in both ^{t}Bu complexes compared to the ^{i}Pr ones, with the other parameters not showing significant differences or trends (i.e. the IR carbonyl stretching frequency (υ_{CO}) for complexes **1-4** is 1903, 1906, 1901, and 1909 cm^{-1} respectively). This suggests that the extra four methyl groups do not play a significant role in the steric environment in the immediate vicinity of the metal center and MLC reactivity effects of **1** and **2** can be validly compared to **3** and **4**.

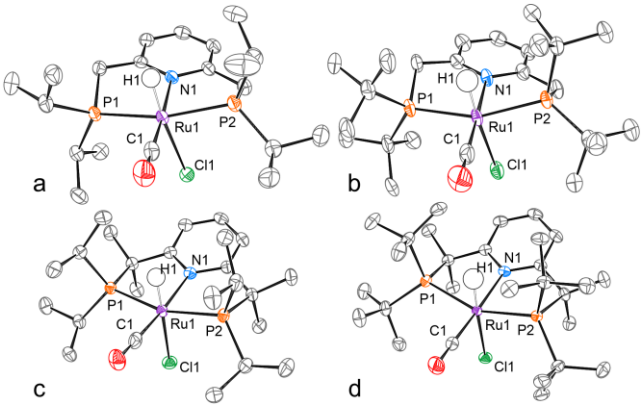

Figure 1. Structures of **1** (a), **2** (b), **3** (c), and **4** (d) in the crystals with thermal ellipsoids at the 70 % probability level. All hydrogen atoms except the [Ru1–]H1 and co-crystallized CH_2Cl_2 molecule in the case of **1** are omitted for clarity. Selected bond distances (Å) and angles (°): Ru1–Cl1 2.5529(4), Ru1–P1 2.3113(4), Ru1–P2 2.3160(5), Ru1–N1 2.1575(15), Ru1–C1 1.838(2), Ru1–H1 1.49(2), P1–Ru1–P2 163.463(18), N1–Ru1–C1 174.83(7) for **1**; Ru1–Cl1 2.5783(7), Ru1–P1 2.3383(8), Ru1–P2 2.3355(7), Ru1–N1 2.142(2), Ru1–C1 1.841(3), Ru1–H1 1.49(4), P1–Ru1–P2 158.37(3), N1–Ru1–C1 178.45(11) for **2**; Ru1–Cl1 2.5659(4), Ru1–P1 2.2956(4), Ru1–P2 2.2993(4), Ru1–N1 2.1625(14), Ru1–C1 1.8371(19), Ru1–H1 1.48(2), P1–Ru1–P2 162.220(17), N1–Ru1–C1 172.88(7) for **3**; Ru1–Cl1 2.5938(3), Ru1–P1 2.3513(3), Ru1–P2 2.3401(3), Ru1–N1 2.1587(9), Ru1–C1 1.8366(12), Ru1–H1 1.527(19), P1–Ru1–P2 156.474(10), N1–Ru1–C1 174.34(4) for **4**.

Synthesis of Ru(0)

We next turned to the synthesis of the desired Ru(0) complexes from **3** and **4**. We reasoned that a strong enough base may be able to deprotonate the complex. KO^{t}Bu did not react with the complexes at room temperature (although complete deprotonation was achieved at higher temperatures and longer time periods). Treating a solution of **3** and **4** in deuterated benzene with the stronger potassium hexamethyl disilazide (KHMDS) gave a red solution after a few minutes, which showed the appearance of a new, symmetrical complex that did not have an associated hydride signal. The reaction was complete after half an hour and we obtained the complexes assigned as Ru(0) **5** and **6** (Scheme 4) based on their NMR spectra, including HMQC correlations and a single ^{31}P NMR peak at 98.3 and 125.3 ppm for **5** and **6**, respectively (see SI). Despite filtering and solvent separation, we could not obtain complexes free of residual HMDS. Complexes **5** and **6** were extremely sensitive to small impurities in solvents or the atmosphere, unsurprisingly also decomposing rapidly in the presence of air and/or water. They could not be stored for prolonged periods of time in the solid state and proved to be unstable in solution after a few days. This was the case regardless of whether the complexes were made and stored under argon or nitrogen, suggesting that there is no stabilization effect from a possible N_2 ligand and that the complexes are tetracoordinate, and have a square planar geometry. Due to this inherent instability, elemental analysis could not be obtained, but sufficient characterization was achieved by NMR and IR spectroscopies. The 16 electron Ru(0) complexes have their aromatic protons shifted significantly upfield. We tried reacting the species with a number of small molecules such as CH_3I, $NO^{+}BF_4^{-}$, or PhI, and in these cases obtained a mixture of products that were not trivial to separate or identify.

In the ^{1}H NMR, complex **5** is well resolved, while the bulkier **6** gives broad signals that begin to resolve at -15°C in toluene-d_8, suggesting hindered rotation, admixture from a paramagnetic state (*vide infra*), or the presence of a relatively long-lived agostic CH interaction between one of the Me groups and the Ru center.

The definite assignment of **5** and **6** as Ru(0) species was aided by their subsequent reactivity with CO and H_2, as these reaction products proved much easier to work with and characterize (Scheme 4).

Reactivity with CO

Putting **5** and **6** under a CO atmosphere led to a fast color change as CO diffused into the solvent, to give dark purple

and dark green solutions, which were determined to contain complexes **7** and **8**, respectively. These product complexes give two carbonyl absorptions in the IR and single peaks in the ^{31}P NMR that are shifted ca. 13 ppm downfield, 113.0 for **7** and 137.9 for **8** compared to the mono-carbonyls, as well as a symmetrical complex ^{1}H NMR pattern.

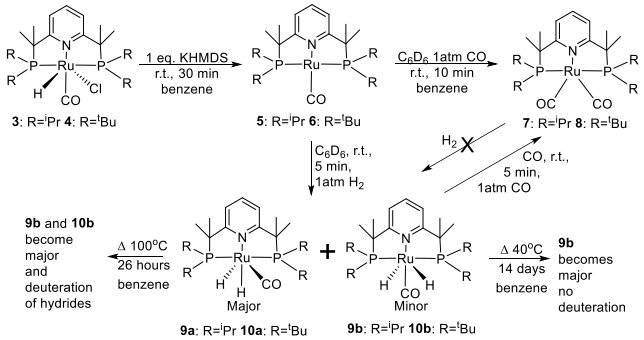

SCHEME 4. Synthesis of Ru(0) complexes and their subsequent reactivity.

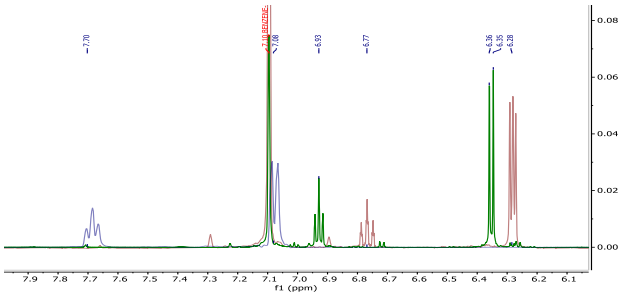

Figure 2. Aromatic NMR shifts of **3** (blue) in THF-d_8, Ru(0) mono CO **5** (green) and Ru(0) bis CO **7** (red) in C_6D_6

In the solid-state, complex **7** adopted a trigonal-bipyramidal geometry, with the two phosphine arms being axial to the CO/N_{Py} plane (Figure 3).

In contrast, the crystal structure of bulkier complex **8** showed that it was a distorted square pyramid. This is an interesting parallel to the low valent Ni(I) oxidation state supported by these same bulky ligands, where the more hindered ^{t}Bu ligand led to the isolation of the square planar PNP-Ni(I)-X motif, while the less bulky ^{i}Pr version allowed for a see-saw structure.[18b] These differences in geometry may mean that another explanation for the broad peaks of **6** is admixture from a paramagnetic state due to the small energy difference between the two higher energy d orbitals, in what may be a highly distorted square planar species.

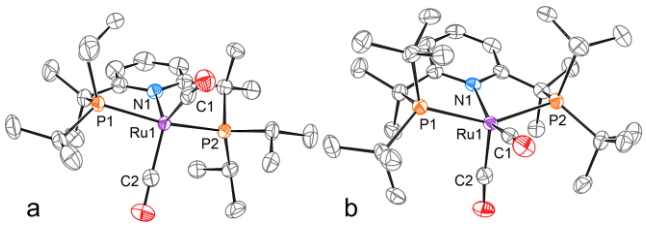

Figure 3. Structures of **7** (a) and **8** (b) in the crystals with thermal ellipsoids at the 70 % probability level. All hydrogen atoms are omitted for clarity. Selected bond distances (Å) and angles (°): Ru1–P1 2.3047(4), Ru1–P2 2.3046(4), Ru1–N1 2.2144(13), Ru1–C1 1.8772(16), Ru1–C2 1.8734(16), O1–C1 1.1717(19), O2–C2 1.173(2), P1–Ru1–P2 160.385(15), N1–Ru1–C1 119.26(6), N1–Ru1–C2 119.57(6) for **7**; Ru1–P1 2.3360(4), Ru1–P2 2.3361(4), Ru1–N1 2.1788(13), Ru1–C1 1.8343(17), Ru1–C2 1.9177(17), O1–C1 1.177(2), O2–C2 1.159(2), P1–Ru1–P2 149.398(14), N1–Ru1–C1 155.13(6), N1–Ru1–C2 98.82(6) for **8**.

The Ru center in **8** is sitting above the basal plane by 0.4948(3) Å; however, the interaction with the axial CO is weaker, with the Ru1-C2 distance being ca. 0.08 Å longer than the distance between Ru and the equatorial carbon. This is also reflected in the longer CO bond length in the equatorial CO at 1.177(2) Å when compared to the axial CO bond length of 1.159(2) Å.

Both bis carbonyl complexes reacted with a number of small molecules, such as MeI or $NO^{+}BF_4^{-}$, but the reactions were not clean and gave a number of undetermined species. These complexes were also stable under an atmosphere of hydrogen gas. As with the mono-carbonyl precursors, exposure to air led to rapid decolorization and decomposition.

Reactivity of 4Me-PNP complexes with H_2

Compounds **5** and **6** could also react with hydrogen to give cis-H_2 complexes **9a** and **10a** (Scheme 4) immediately after H_2 addition. The Ru(0) complexes are not able to heterolytically split the H_2 between the metal center and the ligand (i.e. the MLC mechanism) and can only add the H_2 ligand via homolytic splitting, thus leading to cis-H_2 complexes.

Addition of H_2 to complex **5** is accompanied by a dramatic color change from dark red to light yellow as **9a** is formed. Leaving a sample of **9a** at room temperature does not lead to further changes. However, heating at 100°C for 7 hours leads to significant formation of the trans-H_2 complex and almost complete deuteration of the hydride signals (integration is significantly diminished with respect to aromatic signals and trace Et_2O standard, and an HD isomer shift is observed). This appears to be the equilibrium ratio as a further 19 hours of heating does not show any changes in the spectrum. The cis/trans ratio is difficult to determine due to the deuterium incorporation, with the RuHD and RuD2 complexes leading to some silent ^{1}H NMR signals and broadening in the ^{31}P NMR. Heating the complex at 40°C for two weeks does however lead to the establishment of the same cis/trans equilibrium, without any deuteration of the complex hydrides, or of the dissolved H_2 signal, allowing us to establish a ratio of ~10:1.2 for the trans:cis **9b**:**9a** equilibrium.

Addition of H_2 to complex **6** leads to the formation of **10a** exclusively, which has very broad NMR signals. The hydrides appear as two broad peaks at -6.3 and -13.7 ppm in the ^{1}H NMR. The ^{31}P NMR peak appears in the same general location as the signal of **6** (~125 ppm), but is significantly

broader with a width of ca. 6 ppm for **10a** vs. only a 2 ppm width for **6**. The reaction is accompanied by a color change to dull, light-orange. There is no further reaction at room temperature, but formation of the trans H_2 complex is seen in the ^1H NMR after heating at 100°C for seven hours with the trans complex also being broad and reflecting ca. 18% of all signals. However, it is impossible to determine the ratio with certainty, as there is also a degree of deuteration that takes place at this stage, and the non-hydride signals are too broad and overlapping for accurate integration. A further 19 hours of heating leads to a greater formation of **10b** at the expense of **10a** (~70% being trans assuming equal deuteration as integrated against a trace Et_2O CH_2 signal) and a clear **10b** ^{31}P NMR signal at 138.4 ppm (ca. 1 ppm broad) is also observed.

The above experiments show that the isomerization between the cis and trans dihydride takes place, and that the complexes are capable of regenerating a Ru(0) center that can also activate sp^2 CH/D bonds of the benzene solvent. Although the dihydrides could not be purified by filtration, and under a non H_2 atmosphere were found to slowly lose H_2, leading to the highly unstable complexes **5** and **6**, we were able to isolate crystals of **9b** from an NMR tube reaction (Figure 4), providing a solid-state example of a relatively rare Ru pincer dihydride complex.[1a, 26]

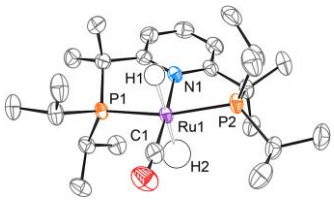

Figure 4. Structure of **9b** in the crystal with thermal ellipsoids at the 70 % probability level. All hydrogen atoms except the [Ru1–]H1 and [Ru1–]H2 and the minor disorder component are omitted for clarity. Selected bond distances (Å) and angles (°): Ru1–P1 2.2707(4), Ru1–P2 2.2968(5), Ru1–N1 2.1608(16), Ru1–C1 1.833(2), Ru1–H1 1.73(2), Ru1–H2 1.73(2), P1–Ru1–P2 162.052(19), N1–Ru1–C1 176.61(7).

Reactivity of dihydride complexes with CO

Replacement of the H_2 atmosphere by CO and heating at 120°C for a few minutes led to the conversion of complexes **9** and **10** to bis carbonyl **7** and **8** according to NMR, accompanied by the characteristic color change to dark purple and green, respectively (Scheme 4). This reaction is not reversible, as also established earlier by the reverse order addition of these gases, and **7** and **8** persisted at room temperature. Addition of the second carbonyl likely occurs via the formation of Ru(0) **5** and **6** from the dihydride complexes.

Reactivity of PNP complexes with H_2

The exclusive initial formation of cis-H_2 with the 4Me-PNP Ru(0) complexes, as well as the subsequent facile deuteration of the hydride signal, can be contrasted to the reactivity of non-methylated complexes **1** and **2**, where addition of base leads to previously reported dearomatized Ru(II) complexes (**11** and **12**, Scheme 5), and the subsequent formation of a trans-H_2 complex, as reported by Milstein.[1a, 26]

It has also been previously reported that addition of substrates such as alcohols,[1a, 26] acids,[6a] carbonyls,[27] and others,[28] leads to addition on the same face of the complex, to both the ligand and the metal. In the case of the addition of H_2, this same-face addition via MLC leads to re-aromatization of the ligand and formation of the trans dihydride complexes **13b** and **14b**. Based on our result with Ru(0) complexes **5** and **6**, we wanted to see if we could observe a putative Ru(0) intermediate that could form the cis dihydride complex, which would subsequently re-arrange to the trans dihydride. However, formation of a cis-H_2 complex is not likely based on the previous examples.

We carefully repeated the H_2 addition experiments to check if a transient cis-H_2 could be detected, however, a few minutes after H_2 addition at r.t. to a C_6D_6 solution, we were unable to observe any traces of cis-H_2 complexes **13a** and **14a** by NMR, with only the trans complex seen. Thus, if the cis-H_2 complexes were formed initially, their re-arrangement to trans dihydrides would have to be much more rapid than in the case of the 4MePNP supported complexes.

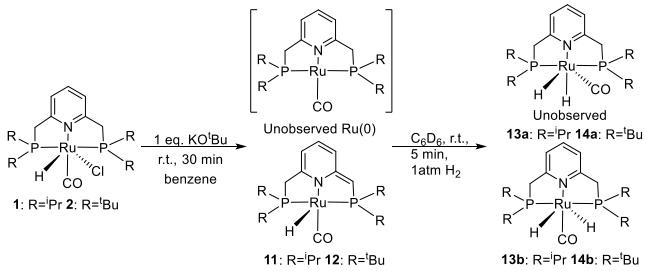

SCHEME 5. Synthesis of non-methylated complexes with base and their subsequent reactivity with H_2.

13b and **14b** exhibited slight deuterium incorporation after several days of heating at 100°C into the hydride signals (ca. 40% deuteration), suggesting the elimination of H_2 and reversible activation of C_6D_6 solvent. However, this is a much lower degree of deuteration than for the 4MePNP complexes (i.e. statistical limit after 7 hours) and after a much longer heating period. We were also unable to observe any traces of the cis complexes at this time, suggesting that there was no observable equilibrium between the trans and cis species if the latter could be accessed at all.

The above observations led us to disfavor formation of the Ru(0) isomer as a viable equilibrium species for PNP based systems, in contrast to 4Me-PNP. The cis/trans hydride ligands' isomerization, and the relatively easy formation of bis-CO complexes from the dihydrides, suggest that catalytically relevant loss of hydrogen can easily occur with the 4MePNP ligand supported complexes. Similarly, the CH activation of the benzene solvent likely occurs via Ru(0) after reductive coupling of the H ligands.

Catalytic reactivity

We investigated the catalytic activity of complexes **1-4** in hexanol and butanol to establish whether the blocking of MLC has a large effect on catalytic activity. The TON was compared against a control experiment with a known, well-performing pre-catalyst H/Cl/CO PNN complex **15**,[9b] which has recently been shown to form a Noyori-type complex in-situ in the reaction mixture (see Figure 1 for structure of activated complex).

Table 1. Activity of complexes **1-4** in ADC.

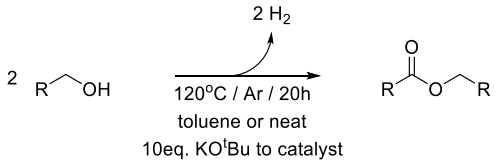

Entry	Complex	Substrate	Substratee qiuv.	Solvent	Conversion (%)	TON
1	15	butanol	3000	neat	86.8	2602 *
2	15	hexanol	3000	neat	51.1	1534 *
3	1	hexanol	1000	toluene	11.4	114
4[a]	1	hexanol	1000	toluene	52.9	367*
5	1	hexanol	3000	neat	6.1	184*
6	1	butanol	3000	neat	5.7	170*
7	2	hexanol	3000	neat	11.4	341*
8	2	butanol	1000	toluene	36.0	360
9	2	butanol	3000	neat	12.4	371
10	3	hexanol	3000	neat	2.0	59*
11	3	butanol	1000	toluene	11.4	114
12	3	butanol	3000	neat	2.6	78
13	4	hexanol	3000	neat	22.4	671*
14	4	butanol	1000	toluene	56.1	561
15	4	butanol	3000	neat	17.5	524

Reactions were performed in about 3.0 ml of total volume of hexanol or 2.4 ml of butanol at 120°C. For reactions in toluene, 1000 eq. of alcohol was used and the volume was raised to 3 ml. Amount of catalyst was calculated according to the substrate. *TON calculated based on an average of at least two runs. a) reaction performed at 157°C.

The reaction was very clean for all five complexes (**1-4**, **15**), with only the starting material and the product present in the NMR after reaction completion. Perhaps somewhat expectedly, the PNN control complex **15** performed best in the reaction with almost complete conversion of butanol and half of all hexanol cleanly converted to the product after 20 hours. The PNP complexes **1-4** all clearly performed worse at the same reaction temperature (120°C). Raising the temperature to 157°C (Entry 4) with complex **1** in toluene to replicate conditions in the original Milstein report, gave a number of byproducts. We determined the identity of the byproducts by GC/MS to be higher alcohols such as dodecanol, likely formed by a Guerbet reaction as reported in a recent paper by the Milstein group.[29] At 157°C, the conversion could thus be calculated based on the integration of all α-CH_2 groups and an accurate TON for hexanol could also determined. Although the TON was ca. 2x higher at the higher temperature, the uncontrolled nature of the reaction is ultimately detrimental as one of the products of the Guerbet reaction is water, which can lead to production of acetate whose coordination is a deactivation pathway for catalysis in the presence of a sub-stoichiometric base.[6a] Indeed, such complexes were later isolated from model experiments (*vide infra*). The temperature was subsequently kept at 120°C to ensure controlled and repeatable catalysis.

Adding toluene as a co-solvent to the reaction did not lead to any appreciable change in TON for any of the complexes, showing that while an open system is required for H_2 escape to drive the reaction, reflux is not necessary. Butanol and hexanol reactivity was compared to judge the effect of solvent polarity and/or substrate size on activity. An assumption can be made that the more polar butanol solvent would stabilize charged intermediates during catalysis, or that a smaller substrate would suffer less from steric hindrance. However, we found that the choice of substrate did not play a role for all four PNP complexes while butanol did indeed give significantly better performance than hexanol in the case of the control PNN complex **15**.

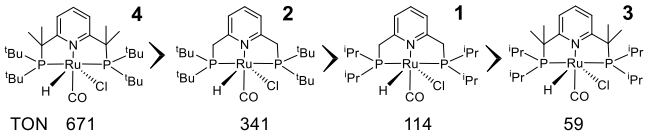

SCHEME 6. Activity of synthesized complexes in catalysis

Surprisingly, besides observing unexpected activity in the 4Me-PNP complexes that were predicted to be inactive in catalysis by MLC, we also observed divergent and unexpected TON trends for all the species. While the worst activity was observed for isopropyl 4Me-PNP complex **3** (entries 10-12), the best catalytic activity was observed for tert-butyl 4Me-PNP **4** (entries 12-15; Table 1). The ^{i}Pr complexes performed significantly worse than the ^{t}Bu complexes, with the most sterically hindered complex **4** reaching 6x as

many TONs as the ^{i}PrPNP Milstein complex **1**. Which, however, in defiance of an easy trend, performed twice better than ^{i}Pr4Me-PNP **3**. The results suggest that the reaction mechanism may differ between the complexes and is not easy to explain generally by traditional MLC. In order to gain insight into the species formed during catalysis, all four complexes were reacted with the model substrate ethanol in NMR experiments with an excess of ethanol in C_6D_6 and also in a neat ethanol solution.

Reactivity with/in ethanol

In 2012, Milstein and Montag investigated the reactivity of **2** at low temperature and found that an activated dearomatized complex in the presence of alcohol formed an alkoxy complex at -80°C, and conversion to an aldehyde and a dihydride complex was already apparent at -30°C.[26] The aldehyde was trapped by the dearomatized complex (Scheme 7). At the time, catalytic activity with this system was not studied at the relevant conditions for catalysis, which would have to include not only experiments with excess alcohol in toluene but also reactions in neat alcohol solvent, as well as heating at catalytically relevant temperatures in order to mimic actual catalytic conditions.

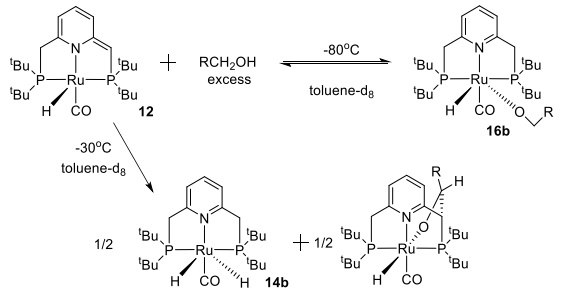

SCHEME 7. Reactivity of ^{t}BuPNP complex **2** and its dearomatized activated complex **12** reported by Milstein.

To append the earlier work, the reactivity of all four complexes **1**-**4** with 5 equivalents of KO^{t}Bu (complexes **1**-**2**) or KHMDS (complexes **3**-**4**) and 40 equivalents of ethanol was observed in a closed system (NMR Young tube) in 0.4 mL of C_6D_6. Alternatively, 0.4 mL of ethanol were used in lieu of deuterated solvent and a solvent suppressed spectrum was obtained. The caveat is that both systems are closed and H_2 gas cannot escape, limiting the ultimate TON. However, formation of ethyl acetate (i.e. ADC catalysis) could still be observed after heating in all but one case; hence the system was treated as a valid proxy for observing catalytic intermediates. NMR spectra were recorded before heating and afterward. The results can be strikingly different depending on the solvent medium, highlighting the need to mimic conditions as close to those of true catalysis as possible in model experiments.

In our NMR experiments, we were able to identify the major complex after each reaction where in one case it is a Noyori-type complex with a hydrogenated backbone and in three cases it is an acetate complex that likely results from a Guerbet reaction that transforms the alcohol substrate to higher alcohols and water. [29] The acetate complexes are thermodynamic sinks that cannot reform an active catalyst without added base. [6a] Thus the TON may depend on the different rate of substrate disproportionation with each complex. Definite conclusions cannot be made due to the complexity of the reactions, as they often involve many organometallic species that are not easy to identify.

Reactivity with EtOH in C_6D_6.

The reactivity with ethanol as an additive in arene solvent is summarized in Scheme 8, and the descriptions of the results for each complex are below.

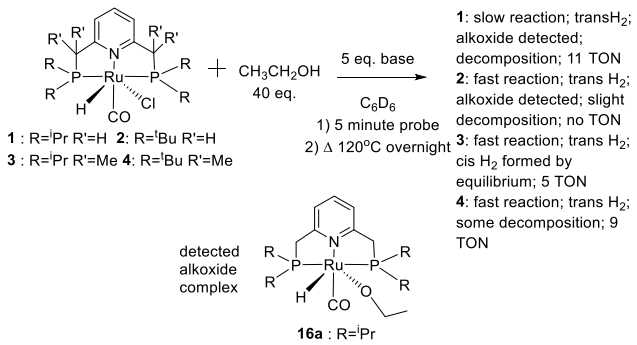

Complex	Catalysis	New Major Species
1	✓	×
2	×	✓
3	✓	×
4	✓	×

SCHEME 8. Summary of reactivity of complexes with 40 eq. ethanol in C_6D_6.

- Complex **1** in C_6D_6 with ethanol additive

Upon adding ethanol to deprotonated ^{i}PrPNP complex **1** in C_6D_6, it immediately formed a mixture of the alkoxy complex **16a** and the trans-H_2 **14a**. After overnight at r.t., dearomatized **11** could not be detected and the **16a**:**14a** ratio was 3:7. After heating at 120°C overnight, the alkoxide **16a** was completely absent, and while **14a** was still the major complex there were eight new symmetrical complex signals in the ^{31}PNMR from 70-89 ppm; none of them the free ligand (Scheme 9). In addition, microcrystals formed on the walls of the NMR tube. There were a number of minor signals in the ^{1}HNMR of the ethanol alpha carbon CH_2 region, but the major ones were still unreacted ethanol and the product of catalysis: ethyl acetate. Dissolved H_2 could also be observed at ca. 4.5 ppm. Without taking into account the reverse ester hydrogenation reaction that should also take place in a closed system, the TON was calculated to be ca. 11.

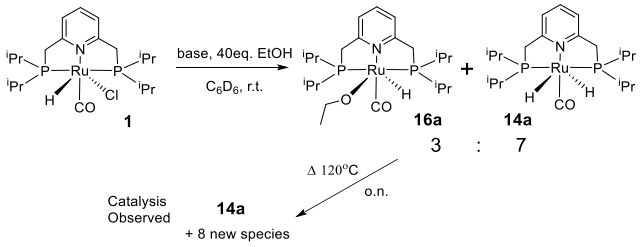

SCHEME 9 Reactivity of complex **1** in C_6D_6 with ethanol

- Complex **2** in C_6D_6 with ethanol additive

For the next complex, ^{t}BuPNP **2**, (and its associated dearomatized **12**) the reactivity exploration would be a continuation of the earlier Milstein mechanistic experiments depicted in Scheme 7. Unlike **1**, addition of ethanol immediately led to the formation of the trans-H_2 **14b** (106.9 ^{31}P NMR shift), with the alkoxy complex **16b** not being detected at room temperature, confirming the earlier Milstein group results [26] and contrasting with the much slower reaction of the ^{i}Pr congener with ethanol (Schemes 9 and 10). Free H_2 could also be observed in solution at this time, and a number of broad peaks in the aromatic region. Heating at 120°C overnight did not change the ^{1}H NMR spectrum significantly, although some new peaks appeared in the ca. 1.2 ppm region and a new minor hydride signal was observed at -26.3 ppm. ^{31}P NMR showed a new minor symmetrical complex peak at 79.1 ppm (later identified as **18**, vide infra). Despite the clean nature of this transformation, EtOAc was not observed (TON ≈ 0). However, complex **2** is a more active catalyst than **1**, suggesting that an open system or a neat ethanol solution is required for catalyst activation.

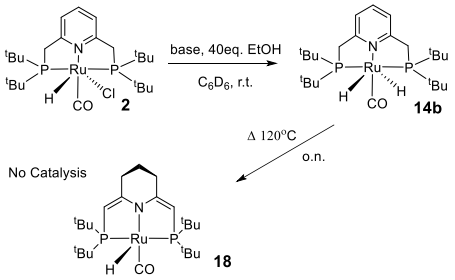

SCHEME 10. Reactivity of complex **2** in C_6D_6 with ethanol

- Complex **3** in C_6D_6 with ethanol additive

The first methylated arm complex ^{i}Pr4MePNP **3**, displayed only the trans-H_2 **9b** 5 minutes after the addition of ethanol in the NMR, although some trace complexes could also be observed in the hydride region. This is a significant contrast to the H_2 addition to the Ru(0) species which gives the cis-H_2 **9a** exclusively. Probing the reaction after 3 hours of heating shows some formation of cis-H_2 **9a**, proving that there is an equilibrium between the two dihydrides, and some ethyl acetate as well as unidentified alcohols. Overnight heating does not significantly change the ratio of **9b**:**9a** (≈ 10:2.3), however, the amount of EtOAc and alcohol byproducts slightly increases with the final TON of ethanol to EtOAc being ca. 5.

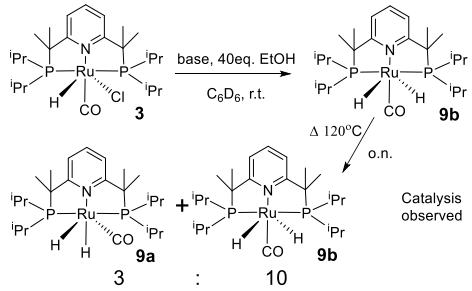

SCHEME 11. Reactivity of complex **3** in C_6D_6 with ethanol

- Complex **4** in C_6D_6 with ethanol additive

The second methylated arm complex ^{t}Bu4MePNP **4**, also gave exclusively the trans-H_2 **10b**, five minutes after mixing it together with base and excess ethanol (Scheme 12). A probe of the reaction a few hours after heating showed that there was some ethyl acetate formed (ca. 6 TON) and that **10b** persisted as the major species, although two new sharp peaks assigned to decomposed ligand, could be identified at 19.5 and 70.8 ppm in the ^{31}P NMR. After heating overnight the decomposition products slightly increased in intensity, and small hydride impurities at ca. -7 ppm also become visible. At this point, the TON for the reaction was ca. 9.

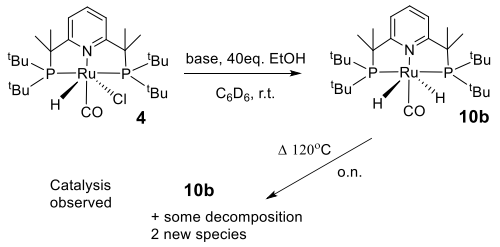

SCHEME 12. Reactivity of complex **4** in C_6D_6 with ethanol

Reactivity in EtOH. (Scheme 13)

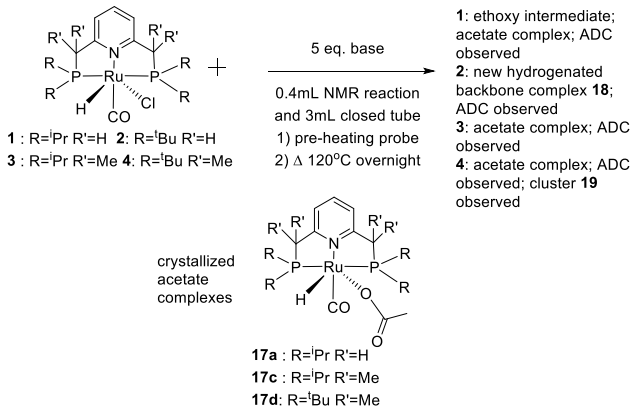

Complex	Catalysis	New Major Species
1	✓	✓
2	✓	✓
3	✓	✓
4	✓	✓

SCHEME 13. Summary of reactivity of complexes in ethanol solution.

The reactivity of **1-4** on a 0.01 to 0.02 mmol scale in 0.4mL. of ethanol was also tested in a Young tube. Due to solvent suppression, the spectra chiefly provided insight in the hydride region of the ^{1}H NMR and in the ^{31}P NMR. The differences with C_6D_6 experiments and added 40 eq. of ethanol are the apparent preference for the alkoxide complex in lieu of the trans-H_2 for **1**, and a greater range of reactivity for all four complexes.

Larger scale reactions at the 0.05 mmol scale were carried out in 3mL. of ethanol in 100mL. Schlenk flasks to isolate products. In some cases, crystallized material formed in a Schlenk flask or NMR tube was used to identify a product. After overnight heating at 120°C in the Schlenk flask, the ethanol was evaporated under high vacuum and the solids were re-dissolved in toluene, filtered through celite, the toluene was evaporated under high vacuum, and NMR obtained in C_6D_6, with the result often being a mixture, but with one major complex predominant. In all four cases, the major complex was crystallized by slow evaporation of toluene or hexane at r.t.

The NMRs obtained after isolating species from Schlenk flask experiments include complexes that formed after decomposition of species that are not stable outside ethanol solvent and/or under vacuum. Another complication is that the shifts in ethanol solvent and those of the species isolated and measured in C_6D_6 cannot be directly compared; however, valuable insight into catalyst decomposition pathways was obtained by crystallizing the main products.

- Complex **1** in ethanol

After adding base to complex **1** dissolved in EtOH, a hydride peak of alkoxide **16a** could be observed in the ^{1}H NMR. After heating overnight **16a** persisted as the major complex, with another two minor symmetrical species appearing as identified by ^{31}P NMR and new hydride shifts; formation of EtOAc and dissolved H_2 could also be confirmed. The Schlenk flask experiment gave an orange solution that contained six ^{31}P NMR peaks (with a new major species at ca. 73 ppm) and as many hydrides. Slow evaporation of hexane led to conversion of the majority of material to orange crystals that gave acetate complex **17a**, assigned to the major species in the NMR (Scheme 14).

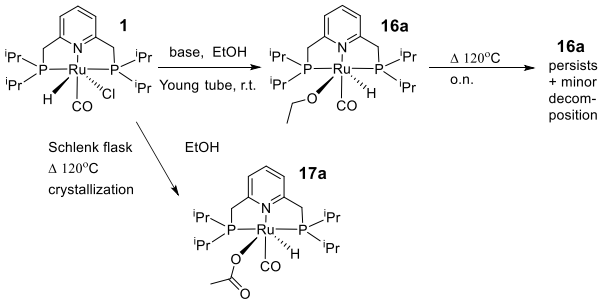

SCHEME 14. Reactivity of complex **1** in neat ethanol

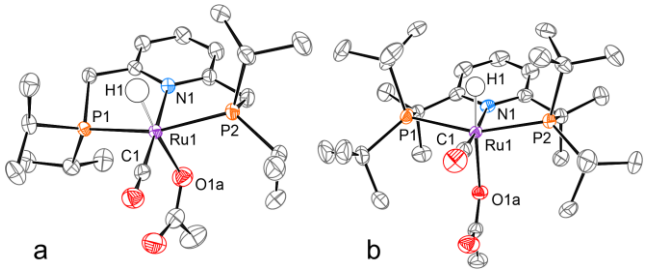

Figure 5. Structures of **17a** (a) and **17d** (b) in the crystals with thermal ellipsoids at the 70 % probability level. All hydrogen atoms except the [Ru1–]H1 are omitted for clarity. Selected bond distances (Å) and angles (°): Ru1–P1 2.3141(3), Ru1–P2 2.3159(3), Ru1–O1a 2.1998(11), Ru1–N1 2.1560(12), Ru1–C1 1.8368(14), Ru1–H1 1.54(2), P1–Ru1–P2 161.084(13), N1–Ru1–C1 176.86(5) for **17a**; Ru1–P1 2.3460(3), Ru1–P2 2.3440(3), Ru1–O1a 2.2160(9), Ru1–N1 2.1704(11), Ru1–C1 1.8332(13), Ru1–H1 1.499(17), P1–Ru1–P2 157.521(12), N1–Ru1–C1 173.55(5) for **17d**. See SI for structure of **17c**.

- Complex **2** in ethanol

Complex **2** after mixing with base and ethanol does not have a changed NMR, with the solution being light yellow, meaning that if deprotonation happened, the starting material could not be differentiated from the alkoxide species under ethanol solvent suppression conditions. After heating for one hour the solution becomes orange; we do not observe the alkoxide **16b** but instead a new major complex with a -26.7 hydride shift (78.7 ppm in ^{31}P NMR). The new complex has no aromatic signals. Another minor complex is present at this time which disappears after overnight heating. After heating the new major complex persists and there are a few trace hydrides. The solution is a brighter orange with orange crystals deposited on the side of the NMR tube. The crystals were analyzed by X-ray diffraction and shown to be the 16 electron Ru complex **18**, where the backbone of the pyridine ring is hydrogenated (Figure 6). However, the arms of the ligand are deprotonated. This type of hydrogenated ligand complex was only obtained from **2** and not the other three complexes. It is easy to propose that complex **18** can catalyze alcohol dehydrogenation in a similar manner to hydrogenated **15** [16] where addition of ethanol leads to protonation of the nitrogen and formation of an alkoxy complex. Unlike the previously published results with **15** however, the associated alkoxy complex **16b** is not detected; indeed, the crystals were *isolated from ethanol* solution!

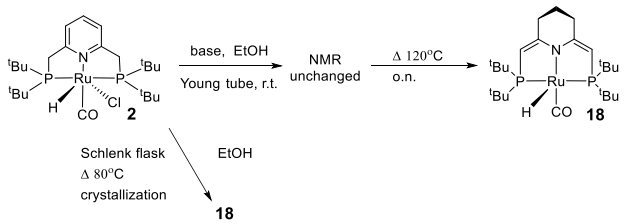

SCHEME 15. Reactivity of complex **2** in neat ethanol

Counterintuitively, complex **18** prefers to be a 16-electron species despite the large concentration of ethanol. This

complex was also observed in the ethanol (vide supra) in C_6D_6 reaction, where it can be detected as a minor complex after overnight heating. That reaction was the only one out of the four that did not show catalytic formation of EtOAc and the only one to have such an extremely upfield shifted hydride peak that only later could be identified as **18**. It's not clear why **2** reacts so differently compared to the other three complexes, but it highlights that small changes in sterics and electronics can cause dramatic changes in catalytic pathways and would also mean that results with one system should not be generalized to all.

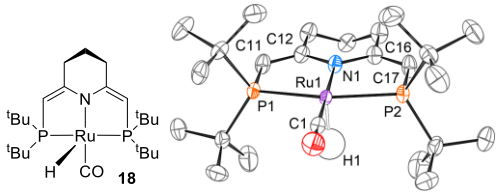

Figure 6. Structure of **18** in the crystal with thermal ellipsoids at the 70 % probability level. All hydrogen atoms except the [Ru1–]H1 and the minor disorder component are omitted for clarity. Selected bond distances (Å) and angles (°): Ru1–P1 2.3380(3), Ru1–P2 2.3298(3), Ru1–N1 2.1155(11), Ru1–C1 1.8377(13), Ru1–H1 1.51(2), C11–C12 1.3570(19), C16–C17 1.363(2), P1–Ru1–P2 163.827(13), N1–Ru1–C1 175.12(5).

The reaction of **2** in the Schlenk flask also gave an orange solution after filtering. After concentration of toluene, NMR showed one of the minor hydrides at -6.7 ppm (87.2 ppm in ^{31}P NMR) made up a significant amount of the mixture and was associated with a number of aromatic peaks. We could not identify this species that is present in a ratio of 2:7 with the major **18**, whereas the latter's peaks could be assigned from the mixture. Slow evaporation of toluene led to the transformation of most of the mixture to orange crystals that once again confirmed the structure of **18**.

Repeating the procedure at a lower temperature (80°C), decanting the ethanol, and washing the crystals with ethanol 2x, gave **18** as a pure species in a ca. 5 mg amount. This sample was used for NMR characterization and to determine the TON in a catalytic experiment. The TON under the conditions of Table 1 for hexanol at 120°C was calculated to be ca. 50, which is much lower than the number obtained for parent complex **1**, but does show that **18** is also a competent, albeit less active, catalyst. This suggests alkoxide **16b** formed, and performed a number of turnovers, before itself being converted to **18**.

- Complex **3** in ethanol

Reaction of the first methylated complex **3** in ethanol solvent (Scheme 16) solution was more ambiguous, albeit slightly cleaner than the reaction with ethanol in C_6D_6. The starting material could not be differentiated from the alkoxy species by NMR in ethanol solution. After one hour of heating, the initial ^{31}PNMR peak at 81.2 ppm decreased in intensity in favor of cis-H_2 **9a** (112.0 ppm) and another complex at 80.4 ppm. It's not clear why the cis-H_2 is present in neat ethanol solution while the trans-H_2 **9b** was exclusively observed in C_6D_6 with ethanol added. This may have to do with the dehydrogenation pathway being affected by an ethanol hydrogen bonding network. After overnight heating, the 81.2 peak persisted. A peak at ~81.5 ppm was assigned to **17c** and there were also two unidentified complexes. EtOAc could also be detected.

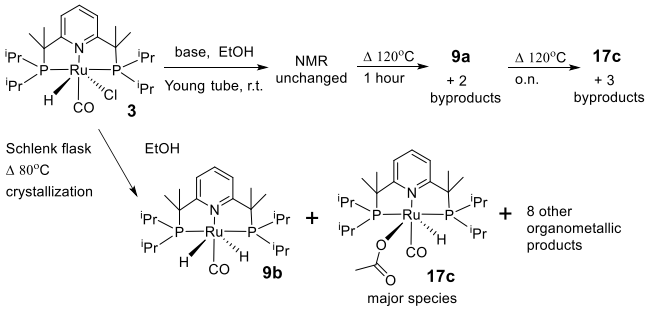

Scheme 16. Reactivity of complex **3** in neat ethanol

After isolation from the Schlenk flask experiment, the NMR revealed three major complexes (and 7 minor ones), with one of the major complexes being trans-H_2 **9b** as its peaks could be matched to the earlier spectra. Since we earlier obtained a crystal structure of **9b** (Figure 4), its greater stability was expected. **9a** was not observed, but this is probably due to facile H_2 elimination under high vacuum via facile reductive coupling. Another of the major complexes was tentatively assigned as the acetate complex based on analogy with **17a**. Slow evaporation of a hexane/toluene mixture of the isolated material led to crystals of acetate complex **17c** and confirmed the assignment.

- Complex **4** in ethanol

Complex **4** (Scheme 17) gave trans-H_2 complex **10b**, after deprotonation in ethanol. Heating for one hour led to a dramatic transformation with two new species being observed: a minor complex with a relatively sharp ~105ppm ^{31}P NMR shift and -5.5 hydride, and the major complex having a broad hydride at -17.3ppm and an associated broad peak centered at the 95 ppm ^{31}P NMR region. After overnight heating **10b** had disappeared completely, and the latter two species persisted. The major complex was assigned to a presumed acetate species **17d** following the earlier pattern of reactivity with complexes **1** and **3**.

The Schlenk flask reaction with **4** led to the formation of yellow crystals on the side of the flask, of which a representative sample could be isolated. For the remaining organometallic compounds (including the majority of the crystals), following ethanol evaporation only ca. 14 mg of material could be obtained after filtration, which was half of the starting material's mass. NMR showed the presence of not less than 10 complexes, with the major one being the acetate complex **17d** and the minor species at ca. 105 ppm seen earlier in the NMR tube reaction. Slow evaporation of a hexane solution led to the conversion of about half of the material to orange crystals of **17d** (Figure 5).

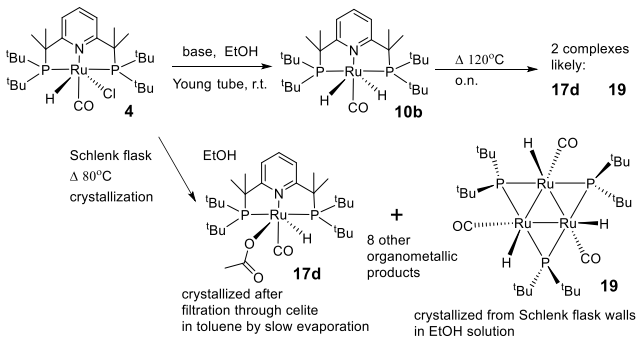

SCHEME 17. Reactivity of complex **4** in neat ethanol

The crystals obtained on the walls of the Schlenk flask were shown to contain a very interesting and unprecedented Ru_3-cluster **19** (Figure 7). This cluster bears some resemblance to the carbonyl/phosphine clusters with bridging hydrides that were explored, including for their catalytic properties, by the groups of Boettcher,[30] Sappa,[31] and others,[32] with the difference being the much lower saturation of Ru centers by phosphine and CO ligands in **19**. It may be of interest for further catalytic exploration due to its high hydride and relatively low CO content. The obvious problem is that it is not clear how to obtain the cluster without it being a decomposition product of **4** in ethanol and we did not obtain enough material to attempt catalysis or to obtain a clean NMR (although a hydride shift at -6.3 ppm (broad triplet) in C_6D_6 could be assigned) before decomposition under air. It's likely that the cluster decomposes under high vacuum, leading to the large number of complexes observed in the residue of the Schlenk flask reaction.

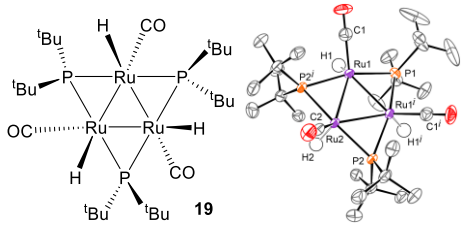

Figure 7. Structure of **19** in the crystal with thermal ellipsoids at the 70 % probability level. All hydrogen atoms except the [Ru1–]H1 and [Ru2–]H2 and the minor disorder component are omitted for clarity. The atoms marked by superscripts *i* are related by the mirror plane (–*x*+1, *y*, *z*). Selected bond distances (Å) and angles (°): Ru1–Ru1^i 2.6656(6), Ru1–Ru2 2.6548(5), Ru1–P1 2.3343(15), Ru1–P2^i 2.3409(12), Ru2–P2 2.3437(11), Ru2–P2^i 2.3437(11), Ru1–C1 1.841(5), Ru2–C2 1.823(8), Ru1–H1 1.40(6), Ru2–H2 1.40(6), Ru2–Ru1–Ru1^i 59.866(9), Ru1–Ru2–Ru1^i 60.269(18), Ru1–P1–Ru1^i 69.63(5), Ru2–P2–Ru1^i 69.04(3).

The cluster could be one of the major decomposition pathways for **4** in ethanol and highlights that the mechanism of catalysis and stability of even the basic architecture of PNP complexes cannot be taken for granted under the reductive catalytic conditions. The decomposition may be aided by the severe steric strain of **4** compared to the other three complexes.

Complex **4** was the best performing catalyst (Table 1) and it may be tempting to assign the credit to **19**, which does not have analogues with the other three complexes. Such a claim would lack basic evidence. Due to the isolation of acetate complex **17d**, the relatively clean NMR tube reactions, and the precedent with complexes **1** and **3**, we currently assign a greater probability to a more traditional, non-cluster catalyzed process for alcohol dehydrogenation with **4**.

Summary of reactivity and catalysis

It was surprising to us that all four methylated and non-methylated complexes were active in ADC catalysis, seemingly abrogating the traditional requirement for the MLC mechanistic pathway. In fact, the most hindered complex **4** with four methyl groups on the arms, was the most active catalyst out of the four, while the worst performing one was its ^{i}Pr substituted cousin **3**. The prolific range of catalytic reactivity is in striking contrast to our earlier result (Scheme 2), which found that addition of just one pyridine methyl moiety on the arm of a PNP complex completely shuts down catalysis by allowing for ligand rearrangement and the formation of a relatively weak Ru-N bond.

Another unexpected result was the different manner in which complex **2** reacts with ethanol in contrast to the other complexes. We were not able to find even a hint of a similar hydrogenated backbone species such as **18**, with its characteristic upfield hydride shift and lack of associated aromatic signals, for the other three complexes. Reactions of complexes **1**, **3**, and **4** led to crystallization of acetate complexes as the major species in Schlenk flask post-reaction mixtures, while the reaction of **2** did not show even a trace of the acetate complex based on a careful examination of the hydride region.

Lastly, complex **4** also decomposed to give upfield shifted ^{31}P NMR peaks that were not observed in the other three reactions, and crystals isolated from an ethanol solution revealed the presence of a novel and unusual cluster species **19**, while the acetate complex was isolated from the toluene soluble residue.

It would be tempting to assign greater reactivity to one particular pathway, such as formation of **19** or **18** as the superior catalyst, while the pathway via traditional MLC is disfavored. However, **18** or **19** were obtained in small amounts and a preliminary test with **18** showed lower catalytic activity than the parent complex **2**. The control reaction with PNN complex **15**, earlier shown by us to proceed via a ligand hydrogenation mechanism and NH bond assistance during catalysis also shows much greater activity than any of the herein tested PNP complexes.

The results from the current study and our earlier two papers, as well as those by others,[21, 33] show that ADC is a versatile reaction that may proceed by several different pathways depending on the complex, or can be completely shut down by a rather trivial ligand modification. In this regard, the presence of acetate complexes formed in super dry ethanol (Supelco, max 1 ppm H_2O), where the maximum water amount present would have been several times less than

the amount of excess base, shows that a Guerbet reaction is an important consideration for catalyst deactivation. As shown previously, excess base allows for trapping of formed acetates and regeneration of the active species.[6a] Designing complexes capable of easily decoordinating acetate, or that are completely inactive in disproportionation, or accepting the necessity of a large excess of base with known catalytic systems that may have performed poorly if activated with only 1-2 eq. of base, may lead to greater TONs.

Conclusion

We synthesized methylated PNP complexes **3** and **4** to test the validity of the metal-ligand cooperative (MLC) catalysis pathway in alcohol dehydrogenation catalysis and compared activity with previously reported non-methylated **1** and **2**. At first, we explored the reactivity of the new complexes and found that we could form 16 and 18 electron Ru(0) species. These are relatively rare, well-defined examples of pincer Ru(0) complexes. We were also able to perform oxidative addition reactions to the 16 electron square planar Ru(0) which gave cis-H_2 complexes as expected from a non-MLC process, while the non-methylated complexes gave trans-H_2 products exclusively.

In comparing ADC catalysis, we found that all four complexes performed differently, and no specific trend could be discerned. In ethanol model reactions, complex **2** was, in contrast to the other three species, uniquely transformed to a hydrogenated backbone complex **18**, which is the first example of a 16 electron Ru(II) complex that is stable in ethanol solution. The other three complexes gave acetate species as the major products, hinting at a common deactivation pathway by alcohol disproportionation (Guerbet process). However, all reactions also gave a number of species that cannot be conclusively identified, highlighted by the isolation of the unusual Ru cluster **19** from solutions of **4**.

Based on the above, we can infer that MLC is not strictly required for ADC and the exact mechanism depends on the complex, with dramatic differences being observed even by slightly changing substituents on the phosphine.

In the future, we would like to synthesize cluster **19** by a different method and test its properties. We are also currently exploring basic organometallic reactions of Ru(0) complexes **5** and **6**. Finally, we also found that blocking of MLC does not mean diminished activity in catalysis. It also allows for more efficient CD activation of benzene solvent and we would like to utilize these bulky ligands for metals which have been shown to be more effective for CH activation reactions and explore further CH functionalization applications.

ASSOCIATED CONTENT

Supporting Information. NMR spectra; IR; full characterization of complexes; reactivity description. This material is available free of charge as an accompanying file on ChemRxiv. CCDC 2079124-2079134, 2079338 contain the supplementary crystallographic data for this paper. These data can be obtained free of charge via www.ccdc.cam.ac.uk/data_request/cif.

AUTHOR INFORMATION

Corresponding Author

* eugenekhaskin@oist.jp

Author Contributions

The manuscript was written through contributions of all authors. / All authors have given approval to the final version of the manuscript.

Funding Sources

The authors would like to acknowledge OIST for funding of the project.

ACKNOWLEDGMENT

The authors acknowledge Professor Dmitry Gusev and Professor Julia Khusnutdinova for valuable discussions and suggestions on the manuscript, and Dr. Michael C. Roy for help with mass spectral measurement. R. R. F. performed crystal structure determination within the statements for Kazan Scientific Center of RAS.

ABBREVIATIONS

ADC, alcohol dehydrogenation catalysis; MLC, metal-ligand cooperation; o.n., overnight

REFERENCES

1. a) Zhang, J.; Leitus, G.; Ben-David, Y.; Milstein, D. Facile Conversion of Alcohols into Esters and Dihydrogen Catalyzed by New Ruthenium Complexes. *Journal of the American Chemical Society* **2005,** *127*, 10840-10841; b) Zhang, J.; Leitus, G.; Ben-David, Y.; Milstein, D. Efficient Homogeneous Catalytic Hydrogenation of Esters to Alcohols. *Angewandte Chemie* **2006,** *118*, 1131-1133; c) Gunanathan, C.; Milstein, D. Applications of Acceptorless Dehydrogenation and Related Transformations in Chemical Synthesis. *Science (Washington, DC, U. S.)* **2013,** *341*, 249; d) Khusnutdinova, J. R.; Milstein, D. Metal-Ligand Cooperation. *Angew. Chem., Int. Ed.* **2015,** *54*, 12236-12273; The following patent by Saudan at. el. describing ester hydrogenation appeared 10 months after the report by the Milstein group in 2006: e) Saudan, L.; Dupau, P.; Riedhauser, J.-J.; Wyss, P. Ruthenium complexes with amine/imine phosphine bidentate ligands for hydrogenation of esters and lactones to give corresponding alcohols or diols. WO2006106483A1, 2006; f) Saudan, L. A.; Saudan, C.; Becieux, C.; Wyss, P. Dihydrogen reduction of carboxylic esters to alcohols under the catalysis of homogeneous ruthenium complexes: high efficiency and unprecedented chemoselectivity. *Angew. Chem., Int. Ed.* **2007,** *46*, 7473-7476.

2. Gunanathan, C.; Ben-David, Y.; Milstein, D. Direct synthesis of amides from alcohols and amines with liberation of H2. *Science (Washington, DC, U. S.)* **2007,** *317*, 790-792.

3. a) Balaraman, E.; Gnanaprakasam, B.; Shimon, L. J. W.; Milstein, D. Direct Hydrogenation of Amides to Alcohols and Amines under Mild Conditions. *J. Am. Chem. Soc.* **2010,** *132*, 16756-16758; b) Cabrero-Antonino, J. R.; Alberico, E.; Drexler, H.-J.; Baumann, W.; Junge, K.; Junge, H.; Beller, M. Efficient Base-Free

Hydrogenation of Amides to Alcohols and Amines Catalyzed by Well-Defined Pincer Imidazolyl-Ruthenium Complexes. *ACS Catal.* **2016,** *6*, 47-54; c) John, J. M.; Bergens, S. H. A Highly Active Catalyst for the Hydrogenation of Amides to Alcohols and Amines. *Angew. Chem., Int. Ed.* **2011,** *50*, 10377-10380, S10377/1-S10377/24; d) Kar, S.; Rauch, M.; Kumar, A.; Leitus, G.; Ben-David, Y.; Milstein, D. Selective Room-Temperature Hydrogenation of Amides to Amines and Alcohols Catalyzed by a Ruthenium Pincer Complex and Mechanistic Insight. *ACS Catal.* **2020,** *10*, 5511-5515; e) Shi, L.; Tan, X.; Long, J.; Xiong, X.; Yang, S.; Xue, P.; Lv, H.; Zhang, X. Direct Catalytic Hydrogenation of Simple Amides: A Highly Efficient Approach from Amides to Amines and Alcohols. *Chem. - Eur. J.* **2017,** *23*, 546-548.

4. a) Gnanaprakasam, B.; Zhang, J.; Milstein, D. Direct synthesis of imines from alcohols and amines with liberation of H2. *Angew. Chem., Int. Ed.* **2010,** *49*, 1468-1471, S1468/1-S1468/7; b) Oldenhuis, N. J.; Dong, V. M.; Guan, Z. Catalytic acceptorless dehydrogenations: Ru-Macho catalyzed construction of amides and imines. *Tetrahedron* **2014,** *70*, 4213-4218.

5. a) Cherepakhin, V.; Williams, T. J. Catalyst Evolution in Ruthenium-Catalyzed Coupling of Amines and Alcohols. *ACS Catal.* **2020,** *10*, 56-65; b) Yang, F.-L.; Wang, Y.-H.; Ni, Y.-F.; Gao, X.; Song, B.; Zhu, X.; Hao, X.-Q. An Efficient Homogenized Ruthenium(II) Pincer Complex for N-Monoalkylation of Amines with Alcohols. *Eur. J. Org. Chem.* **2017,** *2017*, 3481-3486; c) Agrawal, S.; Lenormand, M.; Martin-Matute, B. Selective Alkylation of (Hetero)Aromatic Amines with Alcohols Catalyzed by a Ruthenium Pincer Complex. *Org. Lett.* **2012,** *14*, 1456-1459; d) Balaraman, E.; Srimani, D.; Diskin-Posner, Y.; Milstein, D. Direct Synthesis of Secondary Amines From Alcohols and Ammonia Catalyzed by a Ruthenium Pincer Complex. *Catal. Lett.* **2015,** *145*, 139-144.

6. a) Balaraman, E.; Khaskin, E.; Leitus, G.; Milstein, D. Catalytic transformation of alcohols to carboxylic acid salts and H2 using water as the oxygen atom source. *Nat. Chem.* **2013,** *5*, 122-125; b) Gong, D.; Hu, B.; Chen, D. Bidentate Ru(II)-NC complexes as catalysts for the dehydrogenative reaction from primary alcohols to carboxylic acids. *Dalton Trans.* **2019,** *48*, 8826-8834; c) Liu, H.-M.; Jian, L.; Li, C.; Zhang, C.-C.; Fu, H.-Y.; Zheng, X.-L.; Chen, H.; Li, R.-X. Dehydrogenation of Alcohols to Carboxylic Acid Catalyzed by in Situ-Generated Facial Ruthenium-CPP Complex. *J. Org. Chem.* **2019,** *84*, 9151-9160; d) Garrido-Barros, P.; Funes-Ardoiz, I.; Farras, P.; Gimbert-Surinach, C.; Maseras, F.; Llobet, A. In *Water as an oxygen source for oxidation reactions*, 2018; Georg Thieme Verlag: 2018; pp 63-80; e) Choi, J.-H.; Heim, L. E.; Ahrens, M.; Prechtl, M. H. G. Selective conversion of alcohols in water to carboxylic acids by in situ generated ruthenium trans dihydrido carbonyl PNP complexes. *Dalton Trans.* **2014,** *43*, 17248-17254; f) Dahl, E. W.; Louis-Goff, T.; Szymczak, N. K. Second sphere ligand modifications enable a recyclable catalyst for oxidant-free alcohol oxidation to carboxylates. *Chem. Commun. (Cambridge, U. K.)* **2017,** *53*, 2287-2289; g) Zhang, L.; Nguyen, D. H.; Raffa, G.; Trivelli, X.; Capet, F.; Desset, S.; Paul, S.; Dumeignil, F.; Gauvin, R. M. Catalytic Conversion of Alcohols into Carboxylic Acid Salts in Water: Scope, Recycling, and Mechanistic Insights. *ChemSusChem* **2016,** *9*, 1413-1423.

7. a) Ramakrishnan, S.; Waldie, K. M.; Warnke, I.; De Crisci, A. G.; Batista, V. S.; Waymouth, R. M.; Chidsey, C. E. D. Experimental and Theoretical Study of CO_2 Insertion into Ruthenium Hydride Complexes. *Inorg. Chem.* **2016,** *55*, 1623-1632; b) Wesselbaum, S.; vom Stein, T.; Klankermayer, J.; Leitner, W. Hydrogenation of Carbon Dioxide to Methanol by Using Homogeneous Ruthenium-Phosphine Catalyst. *Angew. Chem., Int. Ed.* **2012,** *51*, 7499-7502, S7499/1-S7499/9.

8. a) Luo, J.; Rauch, M.; Avram, L.; Ben-David, Y.; Milstein, D. Catalytic hydrogenation of thioesters, thiocarbamates, and thioamides. *J. Am. Chem. Soc.* **2020,** *142*, 21628-21633; b) Luo, J.; Rauch, M.; Avram, L.; Diskin-Posner, Y.; Shmul, G.; Ben-David, Y.; Milstein, D. Formation of thioesters by dehydrogenative coupling of thiols and alcohols with H2 evolution. *Nat. Catal.* **2020,** *3*, 887-892; c) Rauch, M.; Luo, J.; Avram, L.; Ben-David, Y.; Milstein, D. Mechanistic Investigations of Ruthenium Catalyzed Dehydrogenative Thioester Synthesis and Thioester Hydrogenation. *ACS Catal.* **2021,** *11*, 2795-2807.

9. a) Chatterjee, B.; Gunanathan, C. Ruthenium Catalyzed Selective α- and α,β-Deuteration of Alcohols Using D2O. *Org. Lett.* **2015,** *17*, 4794-4797; b) Khaskin, E.; Milstein, D. Simple and Efficient Catalytic Reaction for the Selective Deuteration of Alcohols. *ACS Catal.* **2013,** *3*, 448-452.

10. Kaithal, A.; Schmitz, M.; Hoelscher, M.; Leitner, W. Ruthenium(II)-catalyzed β-methylation of alcohols using methanol as C1 source. *ChemCatChem* **2019,** *11*, 5287-5291.

11. a) Khaskin, E.; Milstein, D. Catalytic, oxidant-free, direct olefination of alcohols using Wittig reagents. *Chem. Commun. (Cambridge, U. K.)* **2015,** *51*, 9002-9005; b) Chaudhari, M. B.; Bisht, G. S.; Kumari, P.; Gnanaprakasam, B. Ruthenium-catalyzed direct α-alkylation of amides using alcohols. *Org. Biomol. Chem.* **2016,** *14*, 9215-9220; c) Vojkovsky, T.; Deolka, S.; Stepanova, S.; Roy, M. C.; Khaskin, E. Catalytic Sulfone Upgrading Reaction with Alcohols via Ru(II). *ACS Catal.* **2020,** *10*, 6810-6815.

12. Jankins, T. C.; Fayzullin, R. R.; Khaskin, E. Three-Component [1 + 1 + 1] Cyclopropanation with Ruthenium(II). *Organometallics* **2018,** *37*, 2609-2617.

13. a) Morris, S. A.; Gusev, D. G. Rethinking the Claisen-Tishchenko Reaction. *Angew. Chem., Int. Ed.* **2017,** *56*, 6228-6231; b) Spasyuk, D.; Gusev, D. G. Acceptorless Dehydrogenative Coupling of Ethanol and Hydrogenation of Esters and Imines. *Organometallics* **2012,** *31*, 5239-5242; c) Spasyuk, D.; Smith, S.; Gusev, D. G. Replacing Phosphorus with Sulfur for the Efficient Hydrogenation of Esters. *Angew. Chem., Int. Ed.* **2013,** *52*, 2538-2542; d) Filonenko, G. A.; Aguila, M. J. B.; Schulpen, E. N.; van Putten, R.; Wiecko, J.; Mueller, C.; Lefort, L.; Hensen, E. J. M.; Pidko, E. A. Bis-N-heterocyclic Carbene Aminopincer Ligands Enable High Activity in Ru-Catalyzed Ester Hydrogenation. *J. Am. Chem. Soc.* **2015,** *137*, 7620-7623; e) Fogler, E.; Garg, J. A.; Hu, P.; Leitus, G.; Shimon, L. J. W.; Milstein, D. System with Potential Dual Modes of Metal-Ligand Cooperation: Highly Catalytically Active Pyridine-Based PNNH-Ru Pincer Complexes. *Chem. - Eur. J.* **2014,** *20*, 15727-15731.

14. Goncalves, T. P.; Dutta, I.; Huang, K.-W. Aromaticity in catalysis: metal ligand cooperation via ligand dearomatization and rearomatization. *Chem. Commun. (Cambridge, U. K.)* **2021,** *57*, 3070-3082.

15. a) Langer, R.; Fuchs, I.; Vogt, M.; Balaraman, E.; Diskin-Posner, Y.; Shimon, L. J. W.; Ben-David, Y.; Milstein, D. Stepwise metal-ligand cooperation by a reversible aromatization/deconjugation sequence in ruthenium complexes with a tetradentate phenanthroline-based ligand. *Chem. - Eur. J.* **2013,** *19*, 3407-3414; b) Miura, T.; Held, I. E.; Oishi, S.; Naruto, M.; Saito, S. Catalytic hydrogenation of un-activated amides enabled by hydrogenation of catalyst precursor. *Tetrahedron Lett.* **2013,** *54*, 2674-2678; c) Miura, T.; Naruto, M.; Toda, K.; Shimomura, T.; Saito, S. Multifaceted catalytic hydrogenation of amides via diverse activation of a sterically confined bipyridine-ruthenium framework. *Sci Rep* **2017,** *7*, 1586; d) Dub, P. A.; Gordon, J. C. The

role of the metal-bound N–H functionality in Noyori-type molecular catalysts. *Nature Reviews Chemistry* **2018,** *2*, 396-408.
16. Dawe, L. N.; Karimzadeh-Younjali, M.; Dai, Z.; Khaskin, E.; Gusev, D. G. The Milstein Bipyridyl PNN Pincer Complex of Ruthenium Becomes a Noyori-Type Catalyst under Reducing Conditions. *J. Am. Chem. Soc.* **2020,** *142*, 19510-19522.
17. Deolka, S.; Tarannam, N.; Fayzullin, R. R.; Kozuch, S.; Khaskin, E. Unusual rearrangement of modified PNP ligand based Ru complexes relevant to alcohol dehydrogenation catalysis. *Chem. Commun. (Cambridge, U. K.)* **2019,** 55, 11350-11353.
18. a) Lapointe, S.; Khaskin, E.; Fayzullin, R. R.; Khusnutdinova, J. R. Nickel(II) Complexes with Electron-Rich, Sterically Hindered PNP Pincer Ligands Enable Uncommon Modes of Ligand Dearomatization. *Organometallics* **2019,** *38*, 4433-4447; b) Lapointe, S.; Khaskin, E.; Fayzullin, R. R.; Khusnutdinova, J. R. Stable Nickel(I) Complexes with Electron-Rich, Sterically-Hindered, Innocent PNP Pincer Ligands. *Organometallics* **2019,** *38*, 1581-1594.
19. Kuriyama, W.; Matsumoto, T.; Ogata, O.; Ino, Y.; Aoki, K.; Tanaka, S.; Ishida, K.; Kobayashi, T.; Sayo, N.; Saito, T. Catalytic Hydrogenation of Esters. Development of an Efficient Catalyst and Processes for Synthesising (R)-1,2-Propanediol and 2-(l-Menthoxy)ethanol. *Organic Process Research & Development* **2012,** *16*, 166-171.
20. a) Anaby, A.; Schelwies, M.; Schwaben, J.; Rominger, F.; Hashmi, A. S. K.; Schaub, T. Study of Precatalyst Degradation Leading to the Discovery of a New Ruo Precatalyst for Hydrogenation and Dehydrogenation. *Organometallics* **2018,** *37*, 2193-2201; b) Tindall, D. J.; Menche, M.; Schelwies, M.; Paciello, R. A.; Schaefer, A.; Comba, P.; Rominger, F.; Hashmi, A. S. K.; Schaub, T. Ruo or RuII: A Study on Stabilizing the "Activated" Form of Ru-PNP Complexes with Additional Phosphine Ligands in Alcohol Dehydrogenation and Ester Hydrogenation. *Inorg. Chem.* **2020,** *59*, 5099-5115.
21. He, T.; Buttner, J. C.; Reynolds, E. F.; Pham, J.; Malek, J. C.; Keith, J. M.; Chianese, A. R. Dehydroalkylative Activation of CNN- and PNN-Pincer Ruthenium Catalysts for Ester Hydrogenation. *J. Am. Chem. Soc.* **2019,** *141*, 17404-17413.
22. a) Young, K. J. H.; Lokare, K. S.; Leung, C. H.; Cheng, M.-J.; Nielsen, R. J.; Petasis, N. A.; Goddard, W. A., III; Periana, R. A. Synthesis of osmium and ruthenium complexes bearing dimethyl (S,S)-2,2'-(pyridine-2,6-diyl)-bis-(4,5-dihydrooxazol-4-carboxylate) ligand and application to catalytic H/D exchange. *J. Mol. Catal. A: Chem.* **2011,** *339*, 17-23; b) Hashiguchi, B. G.; Young, K. J. H.; Yousufuddin, M.; Goddard, W. A.; Periana, R. A. Acceleration of Nucleophilic CH Activation by Strongly Basic Solvents. *Journal of the American Chemical Society* **2010,** *132*, 12542-12545.
23. Cannon, J. S.; Zou, L.; Liu, P.; Lan, Y.; O'Leary, D. J.; Houk, K. N.; Grubbs, R. H. Carboxylate-assisted C(sp3)-H activation in olefin metathesis-relevant ruthenium complexes. *J Am Chem Soc* **2014,** *136*, 6733-43.
24. Feng, Y.; Lail, M.; Foley, N. A.; Gunnoe, T. B.; Barakat, K. A.; Cundari, T. R.; Petersen, J. L. Hydrogen-Deuterium Exchange between TpRu(PMe3)(L)X (L = PMe3 and X = OH, OPh, Me, Ph, or NHPh; L = NCMe and X = Ph) and Deuterated Arene Solvents: Evidence for Metal-Mediated Processes. *J. Am. Chem. Soc.* **2006,** *128*, 7982-7994.
25. Eizawa, A.; Nishimura, S.; Arashiba, K.; Nakajima, K.; Nishibayashi, Y. Synthesis of Ruthenium Complexes Bearing PCP-Type Pincer Ligands and Their Application to Direct Synthesis of Imines from Amines and Benzyl Alcohol. *Organometallics* **2018,** *37*, 3086-3092.
26. Montag, M.; Zhang, J.; Milstein, D. Aldehyde Binding through Reversible C-C Coupling with the Pincer Ligand upon Alcohol Dehydrogenation by a PNP-Ruthenium Catalyst. *J. Am. Chem. Soc.* **2012,** *134*, 10325-10328.
27. a) Huff, C. A.; Kampf, J. W.; Sanford, M. S. Reversible carbon–carbon bond formation between carbonyl compounds and a ruthenium pincer complex. *Chemical Communications* **2013,** *49*, 7147; b) Vogt, M.; Nerush, A.; Diskin-Posner, Y.; Ben-David, Y.; Milstein, D. Reversible CO_2 binding triggered by metal–ligand cooperation in a rhenium(i) PNP pincer-type complex and the reaction with dihydrogen. *Chem. Sci.* **2014,** *5*, 2043-2051; c) Filonenko, G. A.; Smykowski, D.; Szyja, B. M.; Li, G.; Szczygieł, J.; Hensen, E. J. M.; Pidko, E. A. Catalytic Hydrogenation of CO_2 to Formates by a Lutidine-Derived Ru–CNC Pincer Complex: Theoretical Insight into the Unrealized Potential. *ACS Catalysis* **2015,** *5*, 1145-1154.
28. a) Khaskin, E.; Iron, M. A.; Shimon, L. J. W.; Zhang, J.; Milstein, D. N-H Activation of Amines and Ammonia by Ru via Metal-Ligand Cooperation. *J. Am. Chem. Soc.* **2010,** *132*, 8542-8543; b) Bootsma, J.; Guo, B.; De Vries, J. G.; Otten, E. Ruthenium Complexes with PNN Pincer Ligands Based on (Chiral) Pyrrolidines: Synthesis, Structure, and Dynamic Stereochemistry. *Organometallics* **2020,** *39*, 544-555; c) Guo, B.; De Vries, J. G.; Otten, E. Hydration of nitriles using a metal–ligand cooperative ruthenium pincer catalyst. *Chemical Science* **2019,** *10*, 10647-10652; d) Eijsink, L. E.; Perdriau, S. C. P.; de Vries, J. G.; Otten, E. Metal-ligand cooperative activation of nitriles by a ruthenium complex with a de-aromatized PNN pincer ligand. *Dalton Trans.* **2016,** *45*, 16033-16039; e) Nerush, A.; Vogt, M.; Gellrich, U.; Leitus, G.; Ben-David, Y.; Milstein, D. Template Catalysis by Metal-Ligand Cooperation. C-C Bond Formation via Conjugate Addition of Non-activated Nitriles under Mild, Base-free Conditions Catalyzed by a Manganese Pincer Complex. *J. Am. Chem. Soc.* **2016,** *138*, 6985-6997; f) Perdriau, S.; Zijlstra, D. S.; Heeres, H. J.; de Vries, J. G.; Otten, E. A Metal-Ligand Cooperative Pathway for Intermolecular Oxa-Michael Additions to Unsaturated Nitriles. *Angew. Chem., Int. Ed.* **2015,** *54*, 4236-4240; g) Sun, Y.; Koehler, C.; Tan, R.; Annibale, V. T.; Song, D. Ester hydrogenation catalyzed by Ru-CNN pincer complexes. *Chemical Communications* **2011,** *47*, 8349; h) Vogt, M.; Nerush, A.; Iron, M. A.; Leitus, G.; Diskin-Posner, Y.; Shimon, L. J. W.; Ben-David, Y.; Milstein, D. Activation of Nitriles by Metal Ligand Cooperation. Reversible Formation of Ketimido- and Enamido-Rhenium PNP Pincer Complexes and Relevance to Catalytic Design. *Journal of the American Chemical Society* **2013,** *135*, 17004-17018; i) Filonenko, G. A.; Cosimi, E.; Lefort, L.; Conley, M. P.; Copéret, C.; Lutz, M.; Hensen, E. J. M.; Pidko, E. A. Lutidine-Derived Ru-CNC Hydrogenation Pincer Catalysts with Versatile Coordination Properties. *ACS Catalysis* **2014,** *4*, 2667-2671.
29. Xie, Y.; Ben-David, Y.; Shimon, L. J. W.; Milstein, D. Highly Efficient Process for Production of Biofuel from Ethanol Catalyzed by Ruthenium Pincer Complexes. *Journal of the American Chemical Society* **2016,** *138*, 9077-9080.
30. a) Bottcher, H.-C.; Graf, M.; Wagner, C. Synthesis and characterization of electron-rich phosphido-bridged clusters. *Phosphorus, Sulfur Silicon Relat. Elem.* **2001,** *168-169*, 509-512; b) Bottcher, H.-C.; Graf, M.; Merzweiler, K.; Bruhn, C. Synthesis and X-ray crystal structure of [Ru3(CO)7(μ-H)(μ-PCy2)3]: reaction with carbon monoxide to the electron-rich cluster [Ru3(CO)9(μ-H)(μ-PCy2)3]. *Polyhedron* **1998,** *17*, 3433-3438; c) Graf, M.; Merzweiler, K.; Bruhn, C.; Bottcher, H.-C. Synthesis of triruthenium clusters containing mixed bridging phosphido ligands: X-ray crystal structures of [Ru3(CO)7(μ-H)(μ-PBu2t)(μ-

PCy2)2] and the electron-deficient complex [Ru3(μ-CO)(CO)5(μ-H)2(μ-PBut2)2(Bu2tPH)]. *J. Organomet. Chem.* **1998,** *553*, 371-378.
31. a) Castiglioni, M.; Giordano, R.; Sappa, E. Phosphine-substituted and phosphido-bridged metal clusters in homogeneous catalysis. I. Synthesis and reactivity of (η5-C5H5)NiM3(μ-H)3(CO)9-nLn(M = Ru, Os, n = 1,2: L = PPh3, PPh2H, PCy3, PEt3) and M3(CO)12-nLn(M = Ru, n = 1-3: L = PPh3, PPh2H, PCy3, PEt3; M = Os, n = 1,2: L = PPh3). *J. Organomet. Chem.* **1988,** *342*, 97-109; b) Castiglioni, M.; Giordano, R.; Sappa, E. Phosphine-substituted and phosphido-bridged metal clusters in homogeneous catalysis. II. Behavior of (η5-C5H5)NiM3(μ-H)3(CO)9-nLn(M = Ru, n = 1, 2, L = PPh3, PCy3; M = Os, n = 1, 2, L = PPh3, PPh2H, PEt3, PCy3), M3(CO)12-nLn (M = Ru, n = 1-3, L = PPh3, PPh2H, PEt3, PCy3; M = Os, n = 1, 2, L = PPh3) and related complexes in the hydrogenation-isomerization of 1,4-pentadiene. *J. Organomet. Chem.* **1988,** *342*, 111-27; c) Castiglioni, M.; Giordano, R.; Sappa, E. Phosphine-substituted and phosphido-bridged clusters in homogeneous catalysis. III. Selective hydrogenation of tert-butylacetylene in the presence of Ru3(CO)12-n(PPh2H)n (n = 2, 3), HRu3(CO)10(μ-PPh2), HRu3(CO)9(μ-PPh2), H2Ru3(CO)8(μ-PPh2)2 and HRu3(CO)7(μ-PPh2)3. Spectroscopic identification of common alkyne-substituted cluster intermediates. *J. Organomet. Chem.* **1989,** *362*, 399-410; d) Castiglioni, M.; Giordano, R.; Sappa, E. Phosphine-substituted and phosphido-bridged metal clusters in homogeneous catalysis. IV. Selective hydrogenation of diphenylacetylene and isomerization of cis-stilbene in the presence of Ru3(CO)12-n(PPh2H)n (n = 2, 3), HRu3(CO)10(μ-PPh2), HRu3(CO)9(μ-PPh2) and HRu3(CO)7(μ-PPh2)3. *J. Organomet. Chem.* **1989,** *369*, 419-31.
32. a) Suss-Fink, G.; Godefroy, I.; Faure, M.; Neels, A.; Stoeckli-Evans, H. Reactions of the cluster anion [HRu3(CO)11]- with dicyclohexylphosphine: synthesis and molecular structure of H2Ru3(CO)8(PCy2)2 and H2Ru3(CO)6(PCy2)2(HPCy2)2. *J. Cluster Sci.* **2001,** *12*, 35-48; b) Cabeza, J. A.; Lahoz, F. J.; Martin, A. Cationic and neutral 50-electron triruthenium carbonyl clusters containing three bridging diphenylphosphido ligands. *Organometallics* **1992,** *11*, 2754-6; c) Field, J. S.; Haines, R. J.; Mulla, F. Condensation and degradation products from the thermolysis reactions of the bridged diphenylphosphido derivatives [Ru3(μ2-PPh2)(μ2-H)(CO)9], [Ru3(μ2-PPh2)2(μ2-H)2(CO)8], [Ru3(μ2-PPh2)3(μ2-H)(CO)7] and [Ru3(μ2-PPh2)3(μ2-H)(CO)6(PPh2H)]. *J. Organomet. Chem.* **1990,** *389*, 227-49; d) Bullock, L. M.; Field, J. S.; Haines, R. J.; Minshall, E.; Moore, M. H.; Mulla, F.; Smit, D. N.; Steer, L. M. Condensation as well as trinuclear products from the reaction of triruthenium dodecacarbonyl with diphenylphosphine. *J. Organomet. Chem.* **1990,** *381*, 429-56; e) Lugan, N.; Lavigne, G.; Bonnet, J. J.; Reau, R.; Neibecker, D.; Tkatchenko, I. Evidence for the lability of a bridging phosphido ligand under hydrogen atmosphere. Reactions of the cluster complex Ru3(μ3-P(C6H5)(C5H4N))(μ-P(C6H5)2)(CO)8. *J. Am. Chem. Soc.* **1988,** *110*, 5369-76; f) Rosen, R. P.; Geoffroy, G. L.; Bueno, C.; Churchill, M. R.; Ortega, R. B. Photoinduced formation of phosphido-bridged clusters derived from Ru3(CO)9(PPh2H)3. Crystal and molecular structure of Ru3(μ-H)(μ-PPh2)3(CO)7. *J. Organomet. Chem.* **1983,** *254*, 89-103.
33. Pham, J.; Jarczyk, C. E.; Reynolds, E. F.; Kelly, S. E.; Kim, T.; He, T.; Keith, J. M.; Chianese, A. R. The key role of the latent N-H group in Milstein's catalyst for ester hydrogenation. *ChemRxiv* **2021**, 1-35.

Investigation of alcohol dehydrogenative coupling catalysis (ADC) in a pincer family

M-L Cooperation:

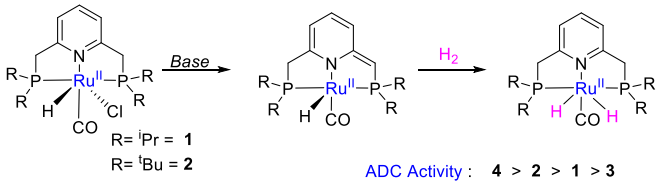

ADC Activity : **4** > **2** > **1** > **3**

TON : 671>341>114>59

Blocking M-L Cooperation:

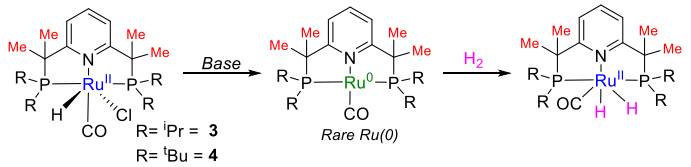

Isolated complexes:

Noyori-type

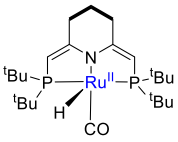

acetate via Guerbet disproportionation